Virology 464-465 (2014) 441–449

Contents lists available at ScienceDirect

Virology

journal homepage: www.elsevier.com/locate/yviro

Characterisation of a novel hypovirus from *Sclerotinia sclerotiorum* potentially representing a new genus within the *Hypoviridae*

Mahmoud E. Khalifa*, Michael N. Pearson

School of Biological Sciences, The University of Auckland, PO Box 92019, Auckland 1010, New Zealand

ARTICLE INFO

Article history:
Received 25 March 2014
Returned to author for revisions
4 May 2014
Accepted 5 July 2014
Available online 6 August 2014

Keywords:
dsRNA
Hypoviridae
Hypovirus
Mycovirus
Sclerotinia sclerotiorum

ABSTRACT

A novel mycovirus tentatively assigned the name Sclerotinia sclerotiorum hypovirus 2 (SsHV2/5472) was detected in the phytopathogenic fungus *Sclerotinia sclerotiorum*. The genome is 14581 nucleotides (nts) long, excluding the poly (A) tail. A papain-like cysteine protease (Pro), an RNA-dependent RNA polymerase (RdRp) and a helicase (Hel) domain were detected in the polyprotein. Phylogenetic analysis based on multiple alignments of the aa sequence of the polyprotein placed it in a distinct clade from *Alphahypovirus* and *Betahypovirus*. The distinct aa sequence plus the fact that SsHV2/5472 possesses the longest reported genome for a hypovirus, suggests that SsHV2/5472 may represent a new genus in the family *Hypoviridae*. Eliminating SsHV2/5472 from *S. sclerotiorum* significantly increased the virulence of the protoplast virus-free derivative 5472-P5, although SsHV/5472-containing isolates showed significant variation in their virulence. In addition, membrane-bound vesicles (25–50 nm) were observed in ultrathin mycelial sections of SsHV2/5472 containing isolates but not in SsHV2/5472-free isolate.

Introduction

Sclerotinia sclerotiorum is a pathogen of over 400 plant species worldwide (Boland and Hall, 1994). Sclerotinia diseases are primarily controlled by fungicides (Bardin and Huang, 2001), the use of which is threatened by the development of fungicide host resistance (Gossen et al., 2001). A range of mycoviruses have been reported to decrease the virulence of *S. sclerotiorum* (Boland, 1992; Khalifa and Pearson, 2013; Xie and Ghabrial, 2012; Xie et al., 2006; Yu et al., 2010) which could potentially be used as an alternative disease biocontrol, similar to that used against chestnut blight (Nuss, 2005).

Mycoviruses with the three reported genome types (single-stranded DNA (ssDNA), double-stranded RNA (dsRNA) and ssRNA) have been reported in *S. sclerotiorum*. According to the ninth report of the International Committee on Taxonomy of Viruses (ICTV) (King et al., 2012), mycoviruses with ssRNA genomes are assigned to families *Metaviridae*, *Pseudoviridae*, *Alphaflexiviridae*, *Gamaflexiviridae*, *Barnaviridae*, *Hypoviridae* and *Narnaviridae*. The *Hypoviridae* includes the extensively studied Cryphonectria hypovirus 1 (CHV1/EP713), which has been successfully used as a biological control agent for the chestnut blight pathogen *Cryphonectria parasitica* (Nuss, 2005).

Polyproteins encoded by hypovirus genomes contain domains similar to those encoded by members of the ssRNA potyviruses infecting plants (Koonin et al., 1991), suggesting the emergence of potyviruses and hypoviruses from a common ancestor. Sequence and phylogenetic analysis of the proteins encoded by members of the *Hypoviridae* led Yaegashi et al. (2012) to propose classification of hypoviruses into two genera, *Alphahypovirus* and *Betahypovirus*, and Wang et al. (2013) to suggest that there might be a gene flow between the two genera.

In this study we present the sequence and molecular characteristics of a novel hypovirus from *S. sclerotiorum* isolate 5472 and its impact on the *in-vitro* growth and virulence of *S. sclerotiorum*. The evolutionary background of the *Hypoviridae* is also analysed and evidence for the role of recombination in their evolution is discussed.

Results

Detection and sequencing of dsRNAs

S. sclerotiorum isolate 5472 contained three distinct dsRNA bands with estimated molecular weights of ~15 kb (dsRNA-L), ~4 kb (dsRNA-M) and ~2 kb (dsRNA-S) (Fig. 1A). All bands resisted digestion by DNase and RNase in high-salt buffer, confirming them to be dsRNAs. Nucleotide sequences were determined using randomly primed RT-PCR and cloning of dsRNA. BLASTX of 22 sequences from dsRNA-L revealed 20 sequences

* Correspondence to: University of Auckland, School of Biological Sciences, Private Bag 92019, Auckland Mail Centre, Auckland, 1142, New Zealand.
Tel.: +64 93737599x87291; Mobile: +64 2102293330; fax: +64 93737416.
E-mail address: mkha201@aucklanduni.ac.nz (M.E. Khalifa).

http://dx.doi.org/10.1016/j.virol.2014.07.005
0042-6822/

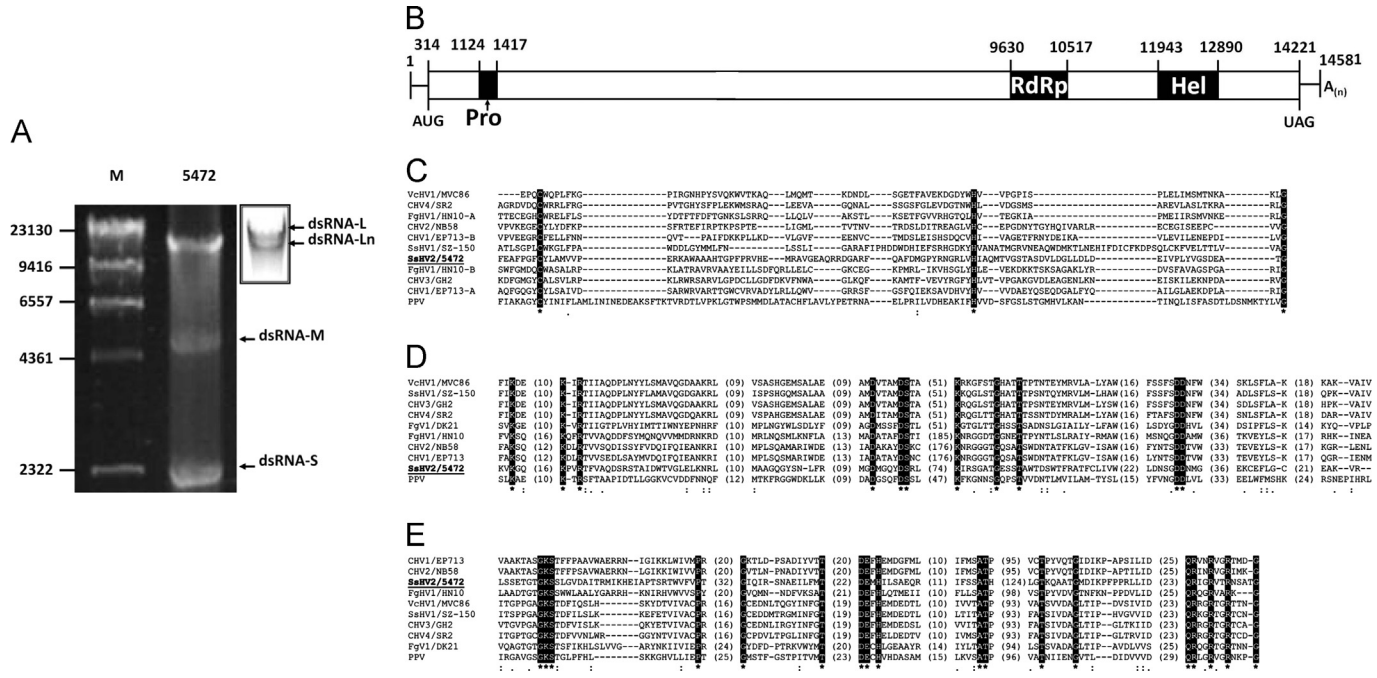

Fig. 1. (A): dsRNA profile of *S. sclerotiorum* isolate 5472. The first lane (M) is DNA molecular weight marker II (Roche, Switzerland). Note: dsRNA-Ln was not initially detected by gel electrophoresis presumably due to its presence in low concentration but detected subsequently by PCR, sequencing, dsRNA extraction and electrophoresis of new subcultures (Inset and Fig. 3). (B): Schematic illustration of SsHV2/5472 genome organisation. (C): aa sequence alignment of SsHV2/5472 Pro domain, domains of other *Hypoviridae* members and that of plum pox virus (PPV). aa sequence alignments of RdRp (D) and Hel (E) domains of SsHV2/5472, *Hypoviridae* members and PPV. Identical residues are dark shadowed and indicated by asterisks "*". Higher and lower chemically similar residues are signified by colons ":" and dots ".", respectively.

with similarities to *Cryphonecteria* hypoviruses (identities 26–27%) and two sequences related to endornaviruses (identities 46–96%). Further separation of dsRNA-L on 0.7% (w/v) agarose gel from several subcultures revealed the presence of a fourth dsRNA (dsRNA-Ln) segment with a molecular weight of ~10 kb (Fig. 1A, inset). Sequences obtained for dsRNA-M showed similarities to unpublished sequences from *S. Sclerotiorum* in GenBank (accession number AHW76811, E-value 0.0, identity 88%; accession number AHE13864, E-value $6e^{-159}$, identity 99% and accession number AHW76812, E-value $1e^{-49}$, identity 66%) and RNA-dependent RNA polymerases (RdRps) of non fungal viruses, including Soybean cyst nematode midway virus (accession number AEF56729, E-value $2e^{-20}$, identity 24%), Nyamanini virus (accession number YP_002905337, E-value $1e^{-14}$, identity 25%) and ebolaviruses. Sequences of dsRNA-S revealed it to be a dsRNA-M-derived defective RNA.

To obtain the complete sequence of dsRNA-L, 112 overlapping clones, obtained by randomly primed RT-PCR were assembled, resulting in three assembled contigs. Sequence gaps were closed by an RT-PCR *fill-in* strategy with specific primers based on the available sequences. The 5′ and 3′ proximal sequences of dsRNA-L were determined by RACE-PCR resulting in a full-length sequence. The mycoviral dsRNA-L was tentatively assigned the name *S. sclerotiorum* hypovirus 2 (SsHV2/5472) and its sequence deposited in GenBank with accession number KF525367.

Molecular characterisation and phylogeny of SsHV2/5472

Sequence analysis of SsHV2/5472 revealed that it is 14581 nts long excluding the poly (A) tail at the 3′ terminus of its positive (+) strand. In reading frame 2, the (+) strand contains a single long open reading frame (ORF) flanked by two untranslated regions (UTRs) at the 5′ and 3′ termini. The ORF consists of 13908 nucleotides (nts) (nt positions 314–14221), initiates at an AUG codon, terminates at an amber termination codon (nt positions 14219–14221) and codes for a polyprotein of 4635 amino acid (aa) residues with a calculated molecular weight of 522.450 kDa. A papain-like cysteine protease (Pro), an RdRp and a helicase (Hel) domain were detected in the polyprotein. No long ORFs were detected on the negative-strand (−) RNA, which is consistent with it being a replicative form of a ssRNA hypovirus. A schematic representation of the genome organisation of SsHV2/5472 is shown in Fig. 1B.

The (+) strand of SsHV2/5472 has a 313 nt long 5′-UTR with multiple upstream AUG codons, similar to those found in CHV1/EP713 and Fusarium graminearum hypovirus 1 (FgHV1/HN10), and has the potential to fold into a complex of stem-loop secondary structures (Supplementary Fig. S1). The full-length 5′-UTR shared low nt identities with those of previously identified members of *Hypoviridae* with a highest identity of 31.5% to Cryphonectria hypovirus 3 (CHV3/GH2). A 3′-UTR of 329 nt (excluding the poly (A) tail), which is the shortest among *Hypoviridae*, showed a highest identity of 23.8% to Cryphonectria hypovirus 4 (CHV4/SR2) when using the full-length 3′-UTRs.

In previous studies, it was reported that stretches of the first and last 100 nts of the 5′- and 3′-UTRs show notable conservation among hypoviruses of the same genus. SsHV2/5472 shared a highest identity of 33% to CHV1/EP713 when the first 100 nts of the 5′-UTRs were used in the alignment. It also shared an identity of 33% to CHV1/EP713 and Valsa ceratosperma hypovirus 1 (VcHV1/MVC86) when using the last 100 nts (excluding the poly (A) tail).

A putative Pro domain consisting of 98 aa residues was detected at the N-terminal end of the polyprotein. As in Pro domains of previously identified *Hypoviridae* members, it contains the conserved cysteine and histidine aa residues (Cys^{278} and His^{333}) required for the autoproteolytic activity and the glycine residue (Gly^{368}) associated with the potential cleavage site (Smart et al., 1999; Yuan and Hillman, 2001) (Fig. 1C). Proteolytic activity of SsHV2/5472 has not been examined using *in-vitro* translational analysis, but the presumed autoproteolytic sites and the putative polyprotein cleavage sites were predicted based on the multiple alignments of SsHV2/5472 Pro domain with those of previously

Table 1
Sequence identities (%) between SsHV2/5472 and other members of *Hypoviridae* based on the multiple alignments of the complete nt sequence, the polyprotein sequence, the nt sequences of the 5′- and 3′-UTRs and aa sequences of different domains.

Virus	Acronym	Full sequence		Non-coding region		Coding region			GenBank accession no.[a]
		nt	aa	5′	3′	Pro	RdRp	Hel	
Cryphonectria hypovirus 1	CHV1/EP713	24.0	12.1[b]	19.8	16.2	20.2/13.1[c]	16.8	25.1	M57938 / AAA67458
Cryphonectria hypovirus 2	CHV2/NB58	27.2	11.3[b]	21.1	15.9	16.2	16.0	23.5	L29010 / AAA20137
Cryphonectria hypovirus 3	CHV3/GH2	27.4	10.8	31.5	14.5	17.2	13.1	14.7	AF188515 / AAF13604
Cryphonectria hypovirus 4	CHV4/SR2	17.6	10.6	17.5	23.8	9.1	14.1	16.9	AY307099 / AAQ76546
Sclerotinia sclerotiorum hypovirus 1	SsHV1/SZ-150	28.8	10.4	19.0	12.9	10.5	12.5	14.1	JF781304 / AEL99352
Valsa ceratosperma hypovirus 1	VcHV1/MVC86	27.0	10.6	26.0	18.9	7.4	14.4	13.2	AB690372 / BAM08994
Fusarium graminearum hypovirus 1	FgHV1/HN10	28.4	12.0[b]	18.1	21.3	11.1/10.1[c]	15.0	22.2	KC330231 / AGC75065

[a] Complete sequence (nt/aa) accession numbers.
[b] aa sequence of ORF-B was used.
[c] Identities to Pro domains of ORF-A and ORF-B are separated by a slash.

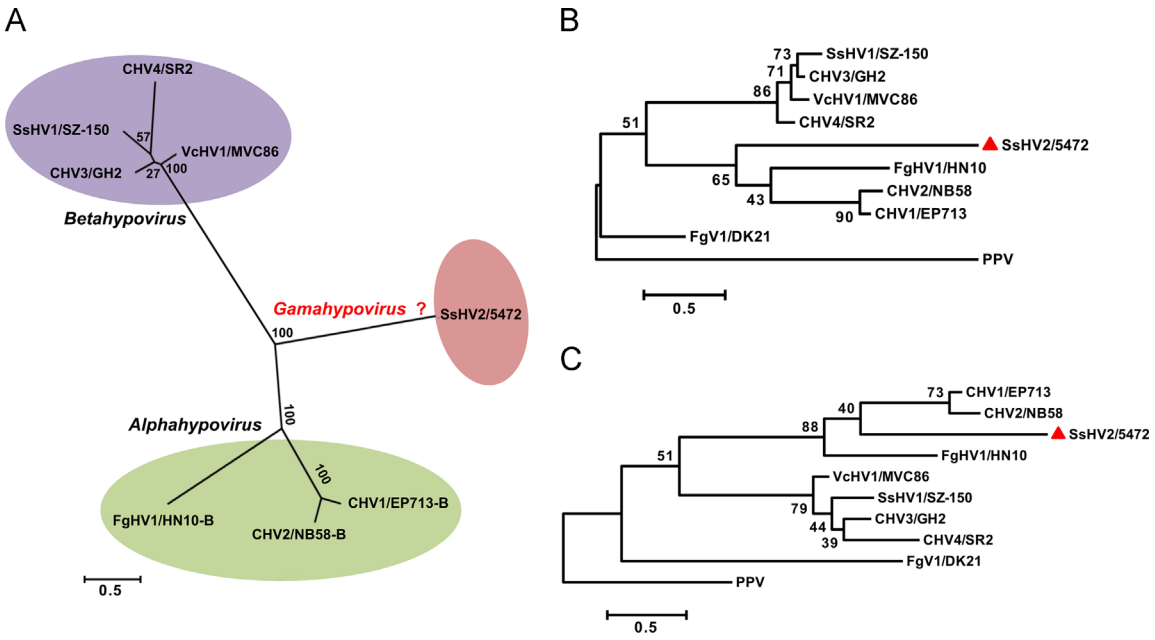

Fig. 2. Maximum likelihood phylogenetic trees based on multiple alignments of (A) polyproteins, (B) RdRp and (C) Hel domains of SsHV2/5472 and other *Hypoviridae* members. Virus notations are as shown in Table 1. To compare the *Hypoviridae* polyproteins, aa sequences of ORF-B were used for CHV1/EP713, CHV2/NB58 and FgHV1/HN10. PPV was used as an outgroup.

described *Hypoviridae* members. The SsHV2/5472 Pro is the closest to that of CHV1/EP713-A (aa identity 20.2%) (Table 1).

An RdRp domain was detected in the polyprotein, downstream from the Pro domain, at aa positions 3106–3401. The SsHV2/5472 RdRp contained the highly conserved aa sequence motifs described for *Hypoviridae* members (Fig. 1D). However the SDD tripeptide which is highly conserved among the members of *Hypoviridae* (Yaegashi et al., 2012) is replaced by GDD in SsHV2/5472 and the *Alphahypovirus* FgHV1/HN10 (Wang et al., 2013) as in most ssRNA viruses (Koonin et al., 1991). Phylogenetic analysis based on the multiple alignments of RdRp domains of *Hypoviridae* members clustered SsHV2/5472 with, but distinctly branched from, members of *Alphahypovirus* (Fig. 2B). Overall SsHV2/5472 shared the highest RdRp aa identity (16.8%) with CHV1/EP713 (Table 1).

A Hel domain was identified at the C-terminal region of the polyprotein, downstream from the RdRp domain, containing the characteristic motifs of the Hel superfamily 2 (Hall and Matson, 1999) with the two conserved DExH and QRxGR boxes at aa positions 3982–3985 (DEMH) and 4180–4184 (QRIGR), respectively (Fig. 1E). SsHV2/5472 displayed identities of 13.2–25.1% to the Hels of *Hypoviridae* members (Table 1) and is most closely related to CHV1/EP713. Phylogenetic analysis based on multiple alignments of Hel domains divided the *Hypoviridae* members into two distinct groups with SsHV2/5472 in the *Alphahypovirus* clade (Fig. 2C).

The phylogenetic trees based on the RdRp and Hel domains divided the members into two clades, separating *Alphahypovirus* from *Betahypovirus* with SsHV2/5472 more closely related to alphahypoviruses. A maximum-likelihood tree of the complete hypoviral polyproteins (Fig. 2A) clearly separated the previously described members of *Alphahypovirus* and *Betahypovirus* into two separate clades while SsHV2/5472 formed a third clade distinct from the currently existing genera. SsHV2/5472 polyprotein shared 10.4–12.1% identity with previously described members of the *Hypoviridae* family (Table 1) whereas identities between members of *Alphahypovirus* and *Betahypovirus* ranged from 9.8% to 11.5%.

Biological properties of isolate 5472 and attempted curing of dsRNA elements

On potato dextrose agar (PDA) plates, SsHV2/5472-infected *S. sclerotiorum* cultures showed apparently normal growth. To assess the effects of SsHV2/5472 on the biological properties of

the fungus, mycelial protoplasting was used to eliminate dsRNAs. Of 48 single protoplast regenerants, 24 were initially screened for viruses using dsRNA analysis and RT-PCR using virus specific primers. As shown in Fig. 3A and B, the single protoplast progeny were divided into four categories based on the dsRNAs present. Group I includes a single isolate (5472-P5) devoid of all four dsRNA segments. Group II has a single isolate (5472-P7) identical to its parent containing all four dsRNA segments. Group III represents the majority of the protoplast progeny (79%) containing a mixture of SsHV2/5472 and dsRNA-Ln and is represented by isolate 5472-P17. Group IV contained three isolates infected with SsHV2/5472 only, represented by isolate 5472-P8.

Effects of dsRNA(s) on host virulence

The 24 protoplast progeny were assessed for their *in-vitro* growth on PDA plates and virulence on detached tomato leaves. The *in-vitro* growth rates did not differ significantly between isolates (data not shown). In contrast, in leaf assays (Fig. 4), after three days, all virus-infected isolates, except 5472-P21, 5472-P23

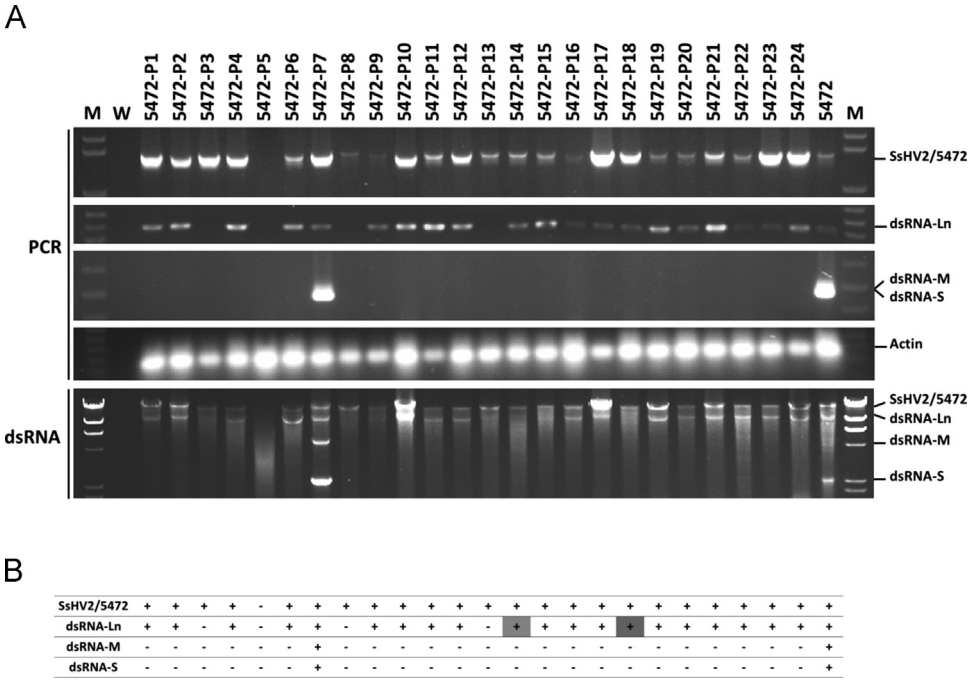

Fig. 3. Regenerant characteristics. (A): Detection of SsHV2/5472 and the other three dsRNAs co-infecting *S. sclerotiorum* isolate 5472 by RT-PCR and dsRNA extraction. 1581, 403, 504 and 504 bp-long fragments were amplified for SsHV2/5472, dsRNA-Ln, dsRNA-M and dsRNA-S, respectively. RT-PCR amplification of *S. sclerotiorum* actin gene (146 bp) was used as an internal control. M: 1 kb Plus DNA Ladder (Invitrogen) (top panel, PCR) and DNA molecular weight marker II (Roche) (bottom panel, dsRNA); W: water negative control. (B): A summary of the virus combinations present in each regenerant (+: present, −: absent). Highlighted boxes indicate that dsRNAs were only detected by PCR and not by dsRNA extraction.

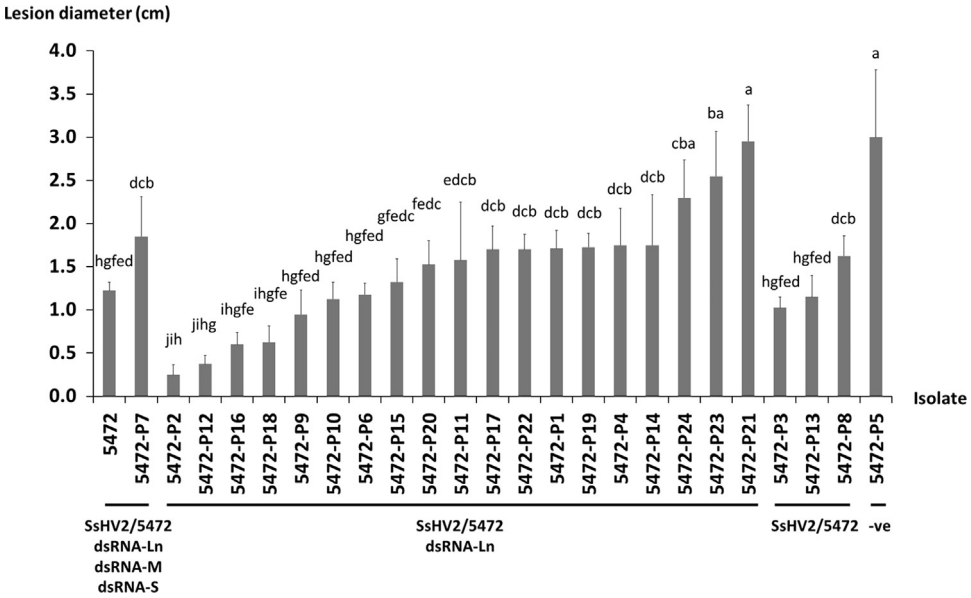

Fig. 4. Lesion diameter comparisons between isolate 5472 and its regenerants. Lesions were measured after a 72-hour incubation period of mycelium plugs on tomato detached leaves and reads are means of four biological replicates. Bars indicate standard error of means and similar letter labels indicate insignificant difference according to the LSD test. Viruses present in each isolate are indicated below the graph and the "−ve" indicates the absence of viruses.

and 5472-P24, showed significant reduction in lesion diameters (0.25–2.55 cm) compared to isolate 5472-P5 (devoid of the 4 dsRNA segments), with a lesion diameter of 3 cm. Isolates with SsHV2/5472 only produced lesions of 0.61–2.02 cm diameter, while isolate 5472-P7, with all four dsRNAs, produced lesions of 1.85 cm in diameter.

Cytological effects of SsHV2/5472

Transmission electron micrographs of the virus-free isolate 5472-P5 showed normal cellular structure with abundant mitochondria and uniform electron density of the cytoplasm (Fig. 5A). In all examined isolates containing SsHV2/5472, either singly or in combination with other viruses, pleomorphic vesicles (25–50 nm) were observed, mostly surrounded by double membranes (Fig. 5B–E). In some sections, virus-containing isolates were vacuolated. No vesicles were observed in isolate 5472-P5 and no differences were spotted between singly and doubly infected fungal progeny.

Recombination analysis and hypovirus evolution

A total of 12 recombination events were detected in five *Hypoviridae* members (Fig. 6) using the Recombination Detection Program (RDP4), which includes several recombination detection

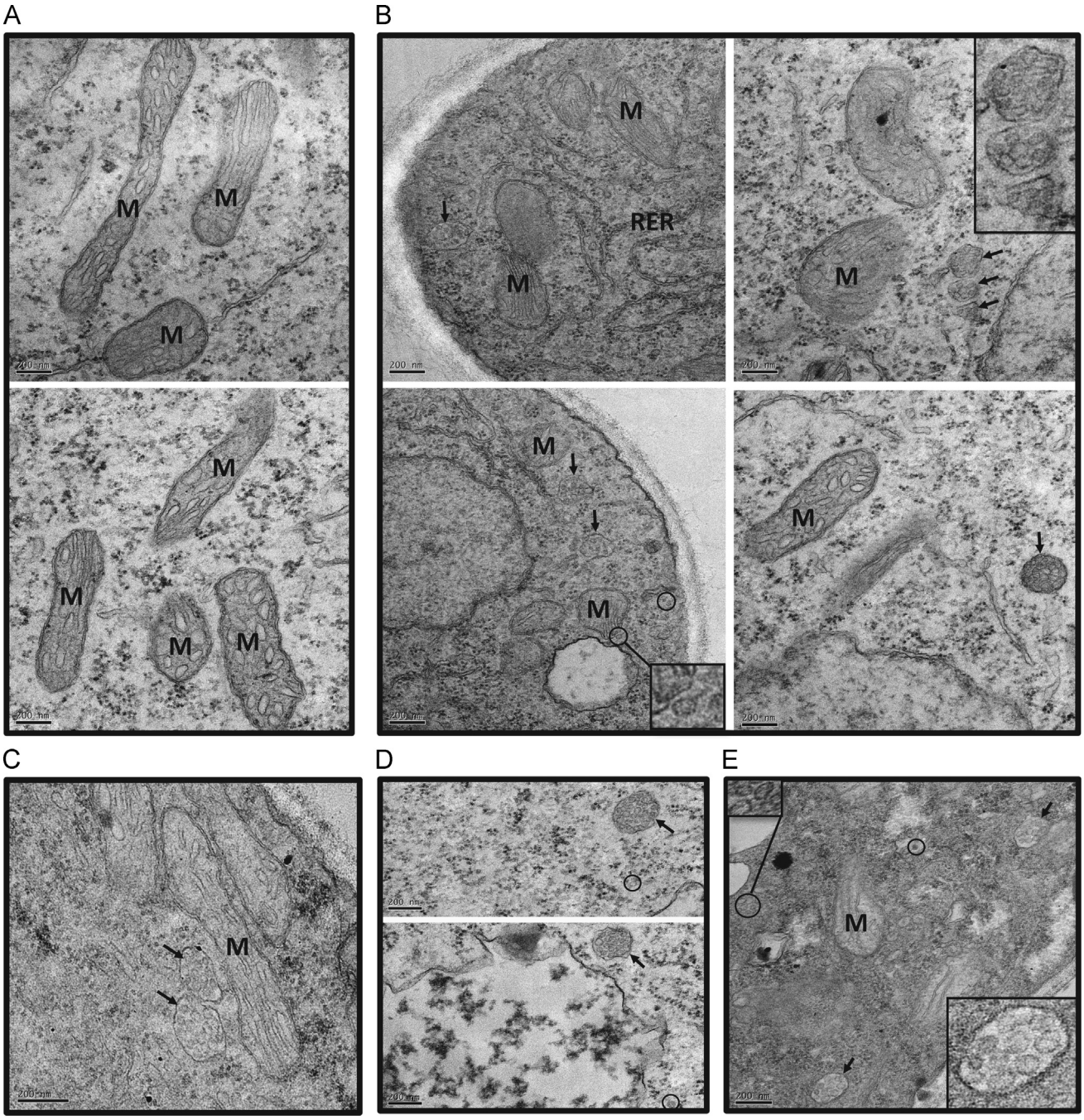

Fig. 5. Transmission electron micrographs showing the cellular structures of (A) *S. sclerotiorum* isolates 5472-P5 (virus free), (B) isolate 5472, (C) isolate 5472-P7, (D) isolate 5472-P8 and (E) isolate 5472-P17. M=mitochondria; RER=rough endoplasmic reticulum. Microvesicles are denoted by circles and multivesicular bodies containing microvesicles are denoted by arrows. Scale bar: 200 nm.

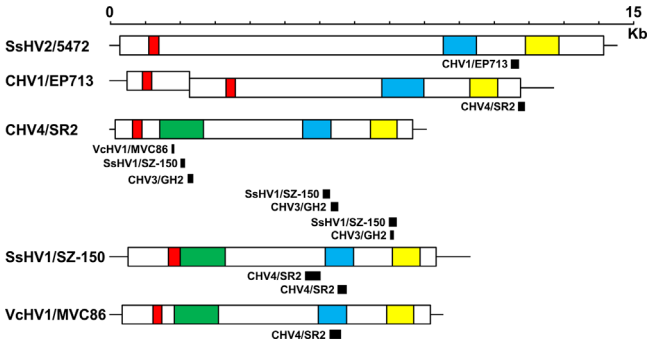

Fig. 6. Hypothesised recombination events in SsHV2/5472 and members of *Hypoviridae* as generated by the RDP4 programme. On the schematic representation of the viral genomes, Pro, UGT, RdRp and Hel domains are represented by red, green, blue and yellow boxes, respectively. Black boxes below each genome indicate hypothesised recombinant regions marked with the name of the minor parents of each recombinant. Virus notations are as shown in Table 1.

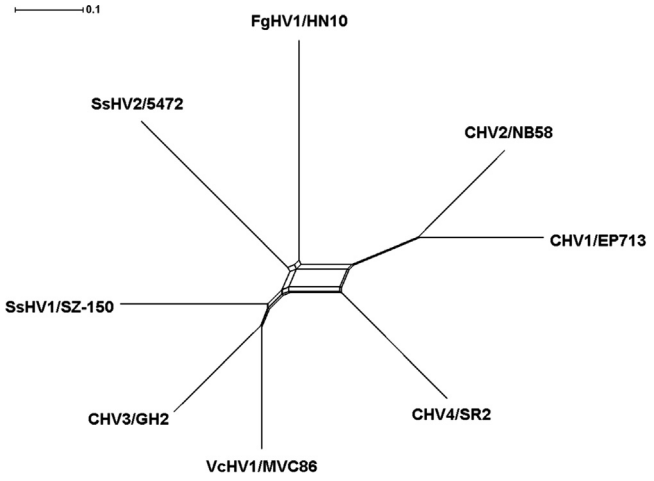

Fig. 7. Splitstree phylogenetic network revealing the evolutionary history of and relationship between SsHV2/5472 and seven members of *Hypoviridae*. Virus notations are as shown in Table 1.

algorithms (Martin et al., 2010). Seven events were detected in CHV4/SR2, two in Sclerotinia sclerotiorum hypovirus 1 (SsHV1/SZ-150), and one event each in SsHV2/5472, CHV1/EP713 and VcHV1/MVC86 (Supplementary Table S1). In CHV4/SR2, six out of seven recombination events (events 2, 3, 4, 5, 7, and 10) were predicted to have major and minor parents from *Alphahypovirus* and *Betahypovirus* genera, respectively. The recombination event localised at nt positions 8078–8176 involved major (SsHV1/SZ-150) and minor (CHV3/GH2) parents that belong to *Betahypovirus*. Recombination events in the closely related betahypoviruses SsHV1/SZ-150 and VcHV1/MVC86 involved the same parental isolates, SsHV2/5472 and CHV4/SR2. In SsHV2/5472, a recombination event was predicted between CHV3/GH2 as a major parent and CHV1/EP713. A recombination event in CHV1/EP713 was detected between Cryphonectria hypovirus 2 (CHV2/NB58) and CHV4/SR2 as major and minor parents, respectively.

The phylogenetic network (Fig. 7) supports the occurrence of recombination events among *Hypoviridae* members or their ancestors and suggests a possible evolutionary history of *Hypoviridae* members. Branches from the central connected reticulate network reflect potential recombination events among the ancestors of the reported members of *Hypoviridae*. Of the five main branches the first includes the alphahypoviruses CHV1/EP713 and CHV2/NB58 which appear to have evolved from the same ancestors and share one recombination event (RDP4 event 6 in Supplementary Table S1). A second branch includes the betahypoviruses CHV3/GH2, SsHV1/SZ-150 and VcHV1/MVC86 which also appear to have diverged from common ancestors. SsHV1/SZ-150 and VcHV1/MVC86 are connected to a series of ancestors including those of SsHV2/5472 and CHV4/SR2, in agreement with the results obtained by RDP4 (events 9, 11 and 12). The most complex recombinant, CHV4/SR2, forms a branch that is connected to the node joining ancestors of isolates in branches 1 and 2. This supports the results obtained by RDP4 that CHV4/SR2 recombination events 2, 3, 4, 5, 7, and 10 (Supplementary Table S1) occurred between ancestors of isolates in branches 1 and 2. The fourth branch accommodates SsHV2/5472 whose ancestors connect isolates from branches 1 and 2, consistent with recombination event 1 (Supplementary Table S1). FgHV1/HN10 forms the fifth branch and indicates that some recombination events have occurred between its ancestors from branches 1, 2 and 4, although no recombination events were detected in FgHV1/HN10 using RDP4. Moreover, the network shows recombination events between all members of *Hypoviridae* or their ancestors (including CHV2/NB58, CHV3/GH2 and FgHV1/HN10) providing evidence of inter-genus recombination events between members or ancestors of *Alphahypovirus* and *Betahypovirus*.

Discussion

Both capsidated and unencapsidated mycoviruses have been reported in *S. sclerotiorum*, often as mixed infections (Jiang et al., 2013), with representatives from all of the non-virion-producing mycoviral families, *Hypoviridae* (Xie et al., 2011), *Narnaviridae* (Khalifa and Pearson, 2013; Xie and Ghabrial, 2012) and *Endornaviridae* (GenBank accession numbers NC_021706 and KJ123645) and the genus *Sclerodarnavirus* (Liu et al., 2009). In this study, a novel hypovirus, provisionally named SsHV2/5472, was detected in a mixed infection with a putative endornavirus and a third virus whose RdRp is similar to those of unpublished sequences from *S. Sclerotiorum*, Ebola, Nyamanini and Midway viruses.

Two genera, *Alphahypovirus* and *Betahypovirus*, whose genomes range in size from ~9 to 13 kb, are currently recognised but have not yet been officially approved within the family *Hypoviridae* (Wang et al., 2013; Yaegashi et al., 2012). In addition to the four hypoviruses from *C. parasitica*, hypoviruses have recently been found in *S. sclerotiorum* (Xie et al., 2011), *Valsa ceratosperma* (Yaegashi et al., 2012) and *Fusarium graminearum* (Wang et al., 2013). Also, another hypovirus from *S. sclerotiorum*, 93% similar to SsHV2/5472 and provisionally named SsHV2/SX247, has been reported (GenBank accession number KJ561218; J. Xie, pers comm.). CHV1 and CHV2 from *C. parasitica* and FgHV1 from *F. graminearum* are assigned to the genus *Alphahypovirus*, whereas CHV3 and CHV4 from *C. parasitica*, SsHV1 from *S. sclerotiorum* and VcHV1 from *V. ceratosperma* are assigned to the genus *Betahypovirus*. Genomes of betahypoviruses consist of a single ORF that encodes a single large polyprotein with a domain that encodes UDP-glucosyltransferase (UGT) and are smaller (9.1–10.4 kb) than alphahypoviruses (12.5–13 kb). *Alphahypovirus* genomes consist of two ORFs and the UGT domain is absent. In contrast SsHV2/5472 does not clearly fit into either *Alphahypovirus or Betahypovirus*. It has a 12% longer genome than FgHV1/HN10, the longest previously reported hypovirus (Wang et al., 2013), and while in common with betahypoviruses with single ORFs, it lacks the UGT, which is a feature of alphahypoviruses. In addition, SsHV2/5472 shows a polyprotein sequence difference (~87.9–89.6%) to members of both *Alphahypovirus* and *Betahypovirus*, which is similar to that between the members of those two genera (~88.5–90.2%), and phylogentic analysis of the polyprotein (Fig. 2A) suggests that SsHV2/5472, together with the isolate SsHV2/SX247 (J. Xie, pers comm.), represents a third distinct lineage and genus, provisionally named *Gamahypovirus*.

Different members of the *Hypoviridae* induce a wide range of phenotypic effects on their hosts. *C. parasitica* isolates infected with CHV1/EP713, CHV2/NB58, and CHV3/GH2 showed reduced virulence (Hillman et al., 1990, 1992, 1994; Smart et al., 1999) whereas CHV4/SR2, SsHV1/SZ150, VcHV1/MVC86 and FgHV1/HN10 produced only mild or no effect on colony morphology and virulence of *C. parasitica* (Linder-Basso et al., 2005), *S. sclerotiorum* (Xie et al., 2011),*V. ceratosperma* (Yaegashi et al., 2012) and *F. graminearum* (Wang et al., 2013), respectively.

Various approaches have been used to separate and eliminate dsRNAs or to obtain virus-free isolates that are isogenic to the parents. In this study, protoplasting and regeneration of single protoplasts successfully eliminated various combinations of the dsRNA elements from the parental 5472 isolate. It is of interest that larger dsRNAs transmitted more efficiently into the protoplasts than smaller dsRNAs, with SsHV2/5472 being present in 96% of the regenerants. One isolate (5472-P5) free of all dsRNAs was obtained and was compared with isolates with various combinations of dsRNAs, including three (5472-P3, 5472-P8 and 5472-P13) that contained only SsHV2/5472. The virus cured isolate showed a significant increase in virulence compared to the virus-containing isolates with the exception of three isolates (5472-P21, -P23 and -P24) that contained SsHV2/5472 and dsRNA-Ln (Fig. 4). The other isolates showed different levels of virulence, the most hypovirulent being isolate 5472-P2, which contained SsHV2/5472 and dsRNA-Ln. Isolates 5472-P3, 5472-P8 and 5472-P13, which contained SsHV2/5472 only, showed very similar levels of virulence and were significantly less virulent than progeny 5472-P5 (devoid of the 4 dsRNAs). The variation in virulence could be due to differences in virus titres in various isolates as was suggested to exist in *Botrytis porri* infected with Botrytis porri RNA virus 1 (BpRV1) (Wu et al., 2012).

Electron microscopy of ultrathin sections of SsHV2/5472-infected isolates showed the presence of 25–50 nm diameter membrane-bound vesicles and multivesicular bodies, which were absent in the SsHV2/5472-free isolate 5472-P5. The vesicle aggregates were often associated with the rough endoplasmic reticulum (RER). Similar spherical, 50–90 nm, membrane-bound vesicles were previously observed in hyphae and conidia of hypovirus-infected *C. parasitica* strains (Newhouse et al., 1983, 1990). Also Nuss and Hillman (2012) reported an association between 50–80 nm pleomorphic vesicles and hypoviral replicative dsRNA and polymerase activity as demonstrated by Fahima et al. (1993). Although the vesicles in this study are smaller than those reported previously, it is possible that different fungal isolates infected with different members of *Hypoviridae* might contain vesicles of various shapes and sizes (Newhouse et al., 1983).

The incongruent phylogenetic relationships between some *Hypoviridae* members in different regions of the genome have previously been noted by Wang et al. (2013), suggesting the occurrence of gene flow through recombination between alphahypoviruses and betahypoviruses. Similarly, recombination events might explain the unique structure of SsHV2/5472, which exhibits some of the properties of both alphahypoviruses and betahypoviruses. Complex evolutionary scenarios and history of a set of taxa cannot be properly reflected by the bifurcating phylogenetic trees, so in order to test this hypothesis we performed a recombination analysis and a phylogenetic network using the available sequences of hypoviruses. When events such as horizontal gene transfer (HGT) and recombination are present, phylogenetic networks should be employed (Huson and Bryant, 2006), as recombination produces reticulate rather than bifurcating trees (Fitch, 1997).

Genetic variations in viruses are generated during virus evolution through mutation, recombination, and reassortment (Domingo and Holland, 1997). Given the large size of *Hypoviridae* genomes, the total number of mutations during the replication is likely to be relatively high and recombination can help to repair defective genomes and maintain functionally adapted RNAs (Allison et al., 1990). Recombination analysis using both RDP4 and the phylogenetic network predicted multiple recombination events between hypoviruses involving parents from both the *Alphahypovirus* and *Betahypovirus*. CHV4/SR2 was identified as the most complex recombinant, carrying seven recombination events. Although FgHV1/HN10 was identified as a non-recombinant isolate by RDP4, the phylogenetic network suggests the emergence of its genome from ancestors with a recombination history between different *Hypoviridae* genera. Supporting evidence for recombination includes the observation of Wang et al. (2013) that the Pro domain of FgHV1/HN10 ORF-B was more closely related to that of CHV1/EP713 ORF-A than -B. Similarly the Pro domain of SsHV2/5472 shared the highest similarity with that in ORF-A of CHV1/EP713. In addition the ungrouping of FgHV1/HN10 and CHV4/SR2 with members of their current genera suggests that they might have a complex evolutionary history involving a series of recombination events among their ancestors. The discovery of new members of *Hypoviridae* in the future may give a clearer picture of their evolutionary history and help to understand the evolution complexity of FgHV1/HN10 and CHV4/SR2.

Materials and methods

Fungal isolate

S. sclerotiorum isolate 5472 was collected in 1969 from an infected *Urtica urens* plant in Hastings, Hawkes Bay, New Zealand. The isolate was subsequently maintained on PDA in the International Collection of Microorganisms from Plants (ICMP) at Landcare Research, Auckland, New Zealand.

DsRNA purification and detection

Extraction of dsRNA was performed using a modified version of the protocol of Valverde et al. (1990). CF-11 cellulose (Whatman, USA) was replaced by MN 301 cellulose (Macherey-Nagel, Germany) which was mixed with the total nucleic acid extract in suspension in the presence of 16% ethanol, rather than passing the sample through cellulose columns as in the original protocol. The cellulose-bound dsRNA was collected by centrifugation at 3000*g* for 3 min and eluted in 6 ml of STE buffer. The dsRNAs were separated by electrophoresis on 0.7% (w/v) agarose gel, in 1 × TAE buffer (pH 7.4), pre-stained with RedSafe (iNtRON, Korea), visualised and photographed under UV using a Gel Doc (Bio-Rad). To confirm the presence of dsRNA the extracted nucleic acid was treated with RQ1 DNase (Promega, USA) and RNase A (Sigma-Aldrich, USA) in both high and low salt conditions as described by Howitt et al. (1995). Nucleic acid molecules that were digested by RNase A in low salt buffer and resisted both DNase and RNase digestion in high salt buffer were considered dsRNA.

cDNA synthesis, PCR, cloning and sequencing

To obtain sequences of dsRNAs, individual dsRNA segments were excised from the agarose gel, extracted using an AxyPrep DNA gel extraction kit (Axygen, USA)and used as templates for cDNA synthesis and PCR amplification. PCR products were cloned into pGEM-T easy vector (Promega, USA) and transformed into *Escherichia coli* DH5α. Subsequent clones were screened and sequenced using T7 and SP6 universal primers.

To determine the terminal sequences, a protocol based on that described by Khalifa and Pearson (2013) was used, but using a SuperScript® III One-Step RT-PCR System with Platinum® Taq DNA Polymerase (Invitrogen, USA) to amplify the terminal sequences (Supplementary materials and methods).

Sequence and phylogenetic analysis

Assembly of nt sequences and translation of ORFs were performed using Geneious Version 5.6.5 (Drummond et al., 2011). Potential ORFs were determined using the National Centre for Biotechnology Information (NCBI) ORF Finder tool (http://www.ncbi.nlm.nih.gov/projects/gorf). Multiple sequence alignments for detection of conserved motifs were carried out using MAFFT version 7 with the default parameters (Katoh and Standley, 2013). Potential secondary structures at the 5′ terminus were predicted using MFOLD software (http://mfold.rna.albany.edu/) (Mathews et al., 1999). Before the phylogenetic analysis was done, multiple sequence alignments were trimmed to ensure all sequences were of the same length. The best-fit substitution models were chosen and maximum likelihood phylogenetic trees constructed using MEGA 5 software (Tamura et al., 2011) with bootstrapping analysis of 1000 replicates. The General Reverse Transcriptase with frequencies and gamma-distributed site rates (rtREV+F+G) was selected for the polyprotein whereas the Whelan and Goldman with gamma-distributed site rates and invariant sites (WAG+G+I) was used for RdRp and Hel.

Curing isolate 5472 of dsRNAs

To determine the effects of the various dsRNA elements on the host fungus it was necessary to eliminate one or more of the dsRNAs. This was achieved by protoplasting and subsequent culturing of single protoplasts. A protocol based on that of Kohn et al. (1990) was used as reported in: http://www.sclerotia.org/lab/protoplasting-sclerotinia-hyphae.

100 μl aliquots of the protoplast suspension were spread uniformly over 20 ml of regeneration media (0.7 M sucrose, 0.5 g/L yeast extract, 15 g/L agar) in petri dishes and incubated at 20 °C for 1–2 days. Single regenerants were transferred onto PDA plates and once the cultures were established, the presence or absence of viruses was determined using dsRNA extraction and RT-PCR.

Detection of viral dsRNAs in single protoplast cultures

Isolate 5472 contained four dsRNAs named dsRNA-L, -Ln, -M and -S. To test for the presence of dsRNAs-L, -M and -S, total RNA was extracted from 100 mg (fresh weight) of fungal mycelium using a Spectrum Plant Total RNA Kit (Sigma-Aldrich, USA) as described by the manufacturer and used for the RT-PCR detection using the SuperScript III One-Step RT-PCR System with Platinum Taq DNA Polymerase kit (Invitrogen, USA) with dsRNA-specific primers (Supplementary Table S2). To test for RT-PCR competency, primers actin-qF2 (5′-GAGCTGTTTTCCCTTCCATTGTC-3′) and actin-qR4 (5′-GACGACACCGTGCTCGATTGG-3′) were used to amplify a 146 bp-long fragment of the *S. sclerotiorum* actin gene (Sexton et al., 2009). Using the above protocol from total RNA, dsRNA-Ln produced only faint bands using primers 5472-LnF and 5472-LnR (Supplementary Table S2). Consequently, purified total dsRNA was used as a template and the same primers used to amplify a 403 bp fragment. Aliquots of dsRNA were mixed with the primers, boiled for 5 min, quickly chilled on ice and used for RT-PCR detection using the one-step kit mentioned above. RT-PCR products were resolved on 1% (w/v) agarose gel in 0.5 × TBE (pH 8.5),pre-stained with RedSafe (iNtRON, Korea), visualised and photographed under UV using a GelDoc (Bio-Rad).

In-vitro growth rate and virulence assays

Fungal isolates were grown on PDA plates for four days at 20 °C and the developing cultures used as inocula to assess the *in-vitro* growth rate and virulence. For *in-vitro* growth rate assessment, 5 mm agar plugs were cut from the actively growing margin, placed at one side of a PDA plate, incubated at 20 °C and the growth measured daily. For the virulence assay, 5 mm agar plugs were cut from the margin of the colony and transferred onto tomato leaves placed on water agar in tissue culture tubs. Tubs were incubated for 72 h at 20 °C in a growth cabinet with a 12 h dark/light cycle. At the end of the incubation period, virulence was assessed by measuring the diameter of the necrotic lesions. Data was analysed as described by Wu et al. (2012) by one-way analysis of variance (ANOVA) using SPSS version 21 (SPSS IBM). Means were compared using the Least Significant Difference (LSD) test. Differences where $P < 0.05$ were considered statistically significant.

Cytological effects of virus infection

Ultrathin sections were prepared and stained using a standard method as described by Khalifa and Pearson (2013). The stained sections were examined using a FEI Tecnai T12 transmission electron microscope.

Recombination detection and construction of a phylogenetic network

Recombination events were analysed using the RDP4 version 4.24, which incorporates a number of recombination detection methods (Martin et al., 2010) including RDP (Martin and Rybicki, 2000), GENECONV (Padidam et al., 1999), BootScan (Martin et al., 2005), MaxChi (Smith, 1992), Chimaera (Posada and Crandall, 2001), SiScan (Gibbs et al., 2000) and 3Seq (Boni et al., 2007); these methods were used in our study with default parameters. Only events predicted by at least three methods, with *P* values < 0.05 and supported phylogenetically, were accepted as recombinants. A split-decomposition phylogenetic network was constructed using the SplitsTree v.4.6 with default parameters (Huson and Bryant, 2006).

Acknowledgement

This research was funded by the Bioprotection Research Centre (Theme 3: Plant Bioprotection Systems Biology; Project 8) and The University of Auckland, New Zealand. We wish to thank Dr. Kar Mun Chooi, The New Zealand Institute for Plant and Food Research, for reading and commenting on the manuscript and the two anonymous reviewers for their valuable comments.

Appendix A. Supporting information

Supplementary data associated with this article can be found in the online version at http://dx.doi.org/10.1016/j.virol.2014.07.005.

References

Allison, R., Thompson, C., Ahlquist, P., 1990. Regeneration of a functional RNA virus genome by recombination between deletion mutants and requirement for cowpea chlorotic mottle virus 3a and coat genes for systemic infection. Proc. Natl. Acad. Sci. U. S. A. 87, 1820–1824.
Bardin, S.D., Huang, H.C., 2001. Research on biology and control of *Sclerotinia* diseases in Canada. Can. J. Plant Pathol. 23, 88–98.
Boland, G.J., 1992. Hypovirulence and double-stranded RNA in *Sclerotinia sclerotiorum*. Can. J. Plant Pathol. 14, 10–17.
Boland, G.J., Hall, R., 1994. Index of plant hosts of *Sclerotinia sclerotiorum*. Can. J. Plant Pathol. 16, 93–108.
Boni, M.F., Posada, D., Feldman, M.W., 2007. An exact nonparametric method for inferring mosaic structure in sequence triplets. Genetics 176, 1035–1047.
Domingo, E., Holland, J.J., 1997. RNA virus mutations and fitness for survival. Annu. Rev. Microbiol. 51, 151–178.
Drummond, A.J., Ashton, B., Buxton, S., Cheung, M., Cooper, A., Duran, C., Field, M., Heled, J., Kearse, M., Markowitz, S., Moir, R., Stones-Havas, S., Sturrock, S.,

Thierer, T., Wilson, A., 2011. Geneious v5.4, Available from ⟨http://www.geneious.com/⟩.
Fahima, T., Kazmierczak, P., Hansen, D.R., Pfeiffer, P., Van Alfen, N.K., 1993. Membrane-associated replication of an unencapsidated double-stranded RNA of the fungus, *Cryphonectria parasitica*. Virology 195, 81–89.
Fitch, W.M., 1997. Networks and viral evolution. J. Mol. Evol. 44, S65–S75.
Gibbs, M.J., Armstrong, J.S., Gibbs, A.J., 2000. Sister-Scanning: a Monte Carlo procedure for assessing signals in recombinant sequences. Bioinformatics 16, 573–582.
Gossen, B.D., Rimmer, S.R., Holley, J.D., 2001. First report of resistance to renomyl fungicide in *Sclerotinia sclerotiorum*. Plant Dis. 85, 1206.
Hall, M.C., Matson, S.W., 1999. Helicase motifs: the engine that powers DNA unwinding. Mol. Microbiol. 34, 867–877.
Hillman, B.I., Halpern, B.T., Brown, M.P., 1994. A viral dsRNA element of the chestnut blight fungus with a distinct genetic organization. Virology 201, 241–250.
Hillman, B.I., Shapira, R., Nuss, D.L., 1990. Hypovirulence-associated suppression of host functions in *Cryphonectria parasitica* can be partially relieved by high light intensity. Phytopathology 80, 950–956.
Hillman, B.I., Tian, Y., Bedker, P.J., Brown, M.P., 1992. A North American hypovirulent isolate of the chestnut blight fungus with European isolate-related dsRNA. J. Gen. Virol. 73, 681–686.
Howitt, R.L.J., Beever, R.E., Pearson, M.N., Forster, R.L.S., 1995. Presence of double-stranded RNA and virus-like particles in *Botrytis cinerea*. Mycol. Res. 99, 1472–1478.
Huson, D.H., Bryant, D., 2006. Application of phylogenetic networks in evolutionary studies. Mol. Biol. Evol. 23, 254–267.
Jiang, D., Fu, Y., Guoqing, L., Ghabrial, S.A., 2013. Viruses of the plant pathogenic fungus *Sclerotinia sclerotiorum*. In: Ghabrial, S. (Ed.), Mycoviruses. Elsevier, San Diego, CA, USA, pp. 215–248.
Katoh, K., Standley, D.M., 2013. MAFFT multiple sequence alignment software version 7: improvements in performance and usability. Mol. Biol. Evol. 30, 772–780.
Khalifa, M.E., Pearson, M.N., 2013. Molecular characterization of three mitoviruses co-infecting a hypovirulent isolate of *Sclerotinia sclerotiorum* fungus. Virology 441, 22–30.
King, A.M.Q., Adams, M.J., Carstens, E.B., Lefkowitz, E.J., 2012. Virus Taxonomy: Classification and Nomenclature of Viruses. Ninth Report of the International Committee on Taxonomy of Viruses. Elsevier Academic Press, London, UK.
Kohn, L.M., Carbone, I., Anderson, J.B., 1990. Mycelial interactions in *Sclerotinia sclerotiorum*. Exp. Mycol. 14, 255–267.
Koonin, E.V., Choi, G.H., Nuss, D.L., Shapira, R., Carrington, J.C., 1991. Evidence for common ancestry of a chestnut blight hypovirulence associated double-stranded RNA and a group of positive-strand RNA plant viruses. Proc. Natl. Acad. Sci. U. S. A. 88, 10647–10651.
Linder-Basso, D., Dynek, J.N., Hillman, B.I., 2005. Genome analysis of *Cryphonectria hypovirus* 4, the most common hypovirus species in North America. Virology 337, 192–203.
Liu, H., Fu, Y., Jiang, D., Li, G., Xie, J., Peng, Y., Yi, X., Ghabrial, S.A., 2009. A novel mycovirus that is related to the human pathogen *Hepatitis E virus* and rubi-like viruses. J. Virol. 83, 1981–1991.
Martin, D., Rybicki, E., 2000. RDP: detection of recombination amongst aligned sequences. Bioinformatics 16, 562–563.
Martin, D.P., Lemey, P., Lott, M., Moulton, V., Posada, D., Lefeuvre, P., 2010. RDP3: a flexible and fast computer program for analyzing recombination. Bioinformatics 26, 2462–2463.
Martin, D.P., Posada, D., Crandall, K.A., Williamson, C., 2005. A modified bootscan algorithm for automated identification of recombinant sequences and recombination breakpoints. AIDS Res. Hum. Retrovir. 21, 98–102.
Mathews, D.H., Sabina, J., Zuker, M., Turner, D.H., 1999. Expanded sequence dependence of thermodynamic parameters improves prediction of RNA secondary structure. J. Mol. Biol. 288, 911–940.
Newhouse, J.R., Hoch, H.C., MacDonald, W.L., 1983. The ultrastructure of *Endothia parasitica*. Comparison of a virulent with a hypovirulent isolate. Can. J. Bot. 61, 389–399.
Newhouse, J.R., MacDonald, W.L., Hoch, H.C., 1990. Virus-like particles in hyphae and conidia of European hypovirulent (dsRNA-containing) strains of *Cryphonectria parasitica*. Can. J. Bot. 68, 90–101.
Nuss, D.L., 2005. Hypovirulence: mycoviruses at the fungal-plant interface. Nat. Rev. Microbiol. 3, 632–642.
Nuss, D.L., Hillman, B.I., 2012. Family *Hypoviridae*. In: King, A.M.Q., Adams, M.J., Carstens, E.B., Lefkowitz, E.J. (Eds.), Virus Taxonomy: Classification and Nomenclature of Viruses. Ninth Report of the International Committee on Taxonomy of Viruses. Elsevier Academic Press, London, UK, pp. 1029–1033.
Padidam, M., Sawyer, S., Fauquet, C.M., 1999. Possible emergence of new geminiviruses by frequent recombination. Virology 265, 218–225.
Posada, D., Crandall, K.A., 2001. Evaluation of methods for detecting recombination from DNA sequences: computer simulations. Proc. Natl. Acad. Sci. U. S. A. 98, 13757–13762.
Sexton, A.C., Minic, Z., Cozijnsen, A.J., Pedras, M.S., Howlett, B.J., 2009. Cloning, purification and characterisation of brassinin glucosyltransferase, a phytoalexin-detoxifying enzyme from the plant pathogen *Sclerotinia sclerotiorum*. Fungal Genet. Biol. 46, 201–209.
Smart, C.D., Yuan, W., Foglia, R., Nuss, D.L., Fulbright, D.W., Hillman, B.I., 1999. *Cryphonectria hypovirus 3*, a virus species in the family *Hypoviridae* with a single open reading frame. Virology 265, 66–73.
Smith, J., 1992. Analyzing the mosaic structure of genes. J. Mol. Evol., 34.
Tamura, K., Peterson, D., Peterson, N., Stecher, G., Nei, M., Kumar, S., 2011. MEGA5: molecular evolutionary genetics analysis using maximum likelihood, evolutionary distance, and maximum parsimony methods. Mol. Biol. Evol. 28, 2731–2739.
Valverde, R.A., Nameth, S.T., Jordan, R.L., 1990. Analysis of double-stranded RNA for plant virus diagnosis. Plant Dis. 74, 255–258.
Wang, S., Kondo, H., Liu, L., Guo, L., Qiu, D., 2013. A novel virus in the family *Hypoviridae* from the plant pathogenic fungus *Fusarium graminearum*. Virus Res. 174, 69–77.
Wu, M., Jin, F., Zhang, J., Yang, L., Jiang, D., Li, G., 2012. Characterization of a novel bipartite double-stranded RNA mycovirus conferring hypovirulence in the phytopathogenic fungus *Botrytis porri*. J. Virol. 86, 6605–6619.
Xie, J., Ghabrial, S.A., 2012. Molecular characterization of two mitoviruses co-infecting a hypovirulent isolate of the plant pathogenic fungus *Sclerotinia sclerotiorum*. Virology 428, 77–85.
Xie, J., Wei, D., Jiang, D., Fu, Y., Li, G., Ghabrial, S., Peng, Y., 2006. Characterization of debilitation-associated mycovirus infecting the plant-pathogenic fungus *Sclerotinia sclerotiorum*. J. Gen. Virol. 87, 241–249.
Xie, J., Xiao, X., Fu, Y., Liu, H., Cheng, J., Ghabrial, S.A., Li, G., Jiang, D., 2011. A novel mycovirus closely related to hypoviruses that infects the plant pathogenic fungus *Sclerotinia sclerotiorum*. Virology 418, 49–56.
Yaegashi, H., Kanematsu, S., Ito, T., 2012. Molecular characterization of a new hypovirus infecting a phytopathogenic fungus, *Valsa ceratosperma*. Virus Res. 165, 143–150.
Yu, X., Li, B., Fu, Y., Jiang, D., Ghabrial, S.A., Li, G., Peng, Y., Xie, J., Cheng, J., Huang, J., Yi, X., 2010. A geminivirus-related DNA mycovirus that confers hypovirulence to a plant pathogenic fungus. Proc. Natl. Acad. Sci. U. S. A. 107, 8387–8392.
Yuan, W., Hillman, B.I., 2001. *In vitro* translational analysis of genomic, defective, and satellite RNAs of *Cryphonectria hypovirus 3-GH2*. Virology 281, 117–123.